Bioorganic & Medicinal Chemistry 17 (2009) 2975–2982

Contents lists available at ScienceDirect

Bioorganic & Medicinal Chemistry

journal homepage: www.elsevier.com/locate/bmc

Identification of novel inhibitors of HCV RNA-dependent RNA polymerase by pharmacophore-based virtual screening and in vitro evaluation

Kisun Ryu [a,†], Nam Doo Kim [a,b,†], Seong Il Choi [c], Cheol Kyu Han [b], Jeong Hyeok Yoon [b], Kyoung Tai No [a], Kyun-Hwan Kim [d,*], Baik L. Seong [a,c,e,*]

[a] Department of Biotechnology, College of Engineering, Yonsei University, Seoul 120-749, Republic of Korea
[b] R&D Center, Equispharm Company, Limited, 3F Sung-ok B/D, 4-1 Sunae-dong, Bundang-gu, Sungnam-shi, Kyunggi-do 463-825, Republic of Korea
[c] Institute of Life Science and Biotechnology, Yonsei University, Seoul 120-749, Republic of Korea
[d] Department of Pharmacology, School of Medicine, and Center for Diagnostic Medicine, Institute of Biomedical Science and Technology, Konkuk University, Seoul 143-701, Republic of Korea
[e] Protheon Incorporated, Yonsei Engineering Research Center B120E, 134 Shinchon-Dong, Seodaemun-Gu, Seoul 120-749, Republic of Korea

ARTICLE INFO

Article history:
Received 14 January 2009
Revised 10 March 2009
Accepted 11 March 2009
Available online 18 March 2009

Keywords:
HCV NS5B, RdRp
Inhibitors
Binding pocket
Virtual screening

ABSTRACT

Hepatitis C virus (HCV) is the major etiological agent of non-A, non-B hepatitis where no effective treatment is available. The HCV NS5B with RNA-dependent RNA polymerase (RdRp) activity is a key target for the treatment of HCV infection. Here we report novel NS5B polymerase inhibitors identified by virtual screening and in vitro evaluation of their inhibitory activities. On the basis of a newly identified binding pocket of NS5B, distinct from the nucleotide binding site but highly conserved among various HCV isolates, we performed virtual screening of compounds that fit this binding pocket from the available chemical database of 3.5 million compounds. The inhibitory activities of the in silico selected 119 compounds were estimated with in vitro RdRp assay. Three compounds with IC50 values of about 20 μM were identified, and their kinetic analyses suggest that these compounds are noncompetitive inhibitors with respect to the ribonucleotide substrate. Furthermore, the single-point mutations of the conserved residues in the binding pocket of NS5B resulted in the significant decrease of the RdRp activity, indicating that the binding pocket presented here might be important for the therapeutic intervention of HCV. These novel inhibitors would be useful for the development of effective anti-HCV agents.

1. Introduction

Hepatitis C virus (HCV) is a positive strand RNA virus of the *Flaviviridae* family.[1] The chronic HCV infection can cause cirrhosis and carcinoma of liver.[2] In order to develop strategies of therapeutic and prophylactic intervention, the structures and functions of the each HCV polyprotein components—C, E1, E2, NS2, NS3, NS4A, NS4B, NS5A, and NS5B—have been extensively studied.[3,4] Among these anti-viral targets, NS5B protein, an RNA-dependent RNA polymerase (RdRp), remains a key target for therapeutic intervention.[5,6] The overall structure of the protein, similar to other RdRp, is composed of three domains including finger, palm, and thumb domains. The HCV NS5B contains unique regions, such as the C-terminal hydrophobic residues and β-hairpin located at the thumb domain.[7,8] The recombinant NS5B proteins obtained either from insect cells or *Escherichia coli* have been successfully employed for its functional and structural characterization.[9–12] The high-resolution three-dimensional crystal structures of the NS5B polymerase is available,[13–15] amenable to the structure-based drug design.

Various nucleoside analog inhibitors are widely used for the treatment of human immunodeficiency virus (HIV), hepatitis B virus (HBV), and herpes simplex virus (HSV).[16,17] A nucleoside analog drug ribavirin is used for the treatment of HCV infected patients.[18] Recently, some nucleoside and nonnucleoside analogs have been tested as the potent candidates of anti-HCV agents.[19–27] However, the effectiveness of nucleoside analogues has been reported to be compromised due to the generation of resistant mutants and the adverse side-effects,[28–30] necessitating the development of new inhibition targets and inhibitors of NS5B. Accordingly, the nonnucleoside inhibitors binding to allosteric sites distinct from the active site have begun to be identified through high throughput screening (HTS) and crystallographic analysis of the inhibitor–NS5B complex.[31–34] Antivirals targeted to non-polymerase of tobacco mosaic virus (TMV) were recently reported as successful inhibitor bound to coat protein.[35] The phenylalanine

* Corresponding authors. Tel.: +82 2 2030 7833; fax: +82 2 2049 6192 (K.H.K); tel.: +82 2 2123 2885; fax: +82 2 392 3582 (B.L.S.).
E-mail addresses: khkim10@kku.ac.kr (K.-H. Kim), blseong@yonsei.ac.kr (B.L. Seong).
† These authors contributed equally to this work.

0968-0896/$ - see front matter © 2009 Elsevier Ltd. All rights reserved.
doi:10.1016/j.bmc.2009.03.024

derivatives and novel racemic compounds, for example, were shown to inhibit the RdRp activity of HCV NS5B by binding to a site 30 Å away from the catalytic center.[32,34] The lead compounds were then further modified and improved for the structure–activity relationship (SAR).[36–38]

The structure-based inhibitor design is one of the practical and powerful methods for the identification of lead compounds for target proteins.[25,39–42] In this study, we identified a potential allosteric site of HCV NS5B that is located in the interface between thumb and palm domains, distinct from the catalytic center. Targeted to this site, the candidate inhibitor compounds fit for this pharmacophore were virtually screened using the commercially available 3-D multiple conformer chemical database PharmoDB™ (Equispharm, Korea). Through the virtual screening, the compound library was down-sized from 3.5 millions to 119 chemicals. The inhibitory activities of the selected compounds were tested by the in vitro RdRp assay, and further kinetic analyses were performed for the hit compounds with a view to develop anti-HCV agents.

2. Results

2.1. Identification of potential allosteric binding pocket

For virtual screening of HCV NS5B target inhibitors, we initially investigated the potential inhibitor binding pockets. There have been several X-ray crystal structures of HCV NS5B-inhibitor complex, in which the inhibitors of nonnucleoside analogues bind the sites, apart from the catalytic center of NS5B.[26,31–34] The proposed template-primer complex model of HCV NS5B for viral replication suggests that the rearrangement of the thumb domain occurs upon RNA binding.[14] A modest movement of the thumb domain would be necessary for the entry of the primer because there does not appear enough space for an RNA double strand. Our rationale in this study is that the small molecules that block the conformational change of the thumb domain can inhibit the RNA replication. With this in view, a plausible pharmacophore was built that ensure interaction with amino acid residues constituting the pocket, using PharmoMap™ (Equispharm, Korea), a software package that has built all feature-based pharmacophore, in which the pharmacophoric points are represented by chemical features such as hydrogen bond acceptors/donors or hydrophobic features.

As a result of the analysis of possible inhibitor binding pocket, we found that the thumb and palm domain interface is a promising inhibitor binding pocket. This pocket includes the following residues such as Pro 197, Arg 200, Val 201, Cys 366, Ser 368, Tyr 383, Leu 384, Met 414, Tyr 415, His 467, and Tyr 448 (Fig. 1A). Then, a pharmacophore map was generated using PharmoMap™ for structure-based virtual screening. As shown in Figure 1B, the pharmacophore features, including hydrogen donors/acceptors and hydrophobic interactions, are illustrated. This pharmacophore features are located with near primer-grip, constituted of Cys 366 and Ser 367, far apart from the catalytic site of HCV NS5B. Therefore, it is unlikely that the virtual screening hit compounds can directly interfere with the catalytic site.

2.2. Virtual screening of compounds fitting the pharmacophore of HCV NS5B

The pharmacophore model was used as a search query for identifying inhibitors from 3-D small molecule database, a commercially available multi-conformer 3-D database comprising 3.5 million compounds (PharmoDB™, Equispharm, Korea). We carried out virtual screening of these compounds suitable for HCV NS5B plausible allosteric binding pocket using PharmoScan™ system, a structure-based virtual screening tool of Equispharm, Korea. The

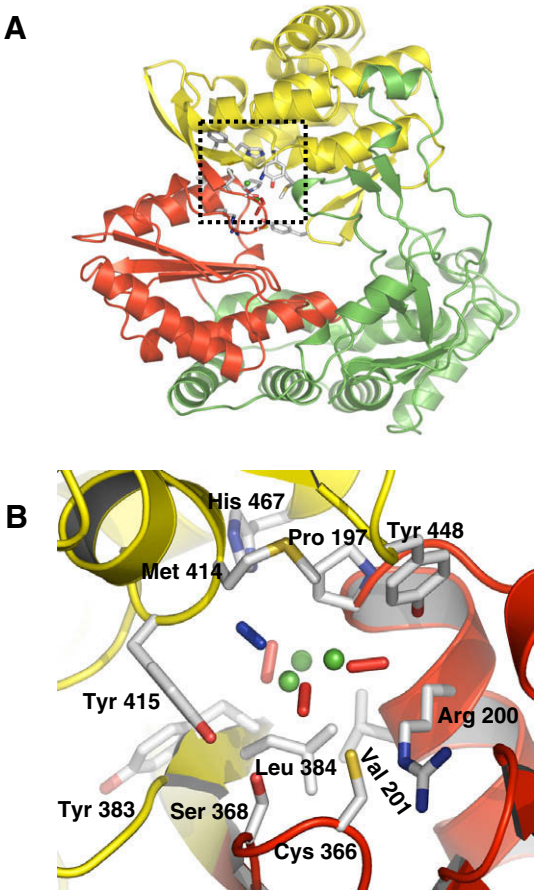

Figure 1. The pharmacophore of HCV NS5B allosteric inhibitor binding site. (A) The overall structure of HCV NS5B and the proposed pharmacophore. The proposed pharmacophore presented with dotted box was located in the interface between the thumb and palm domains of HCV NS5B. The green, red, and blue color represents finger, palm, and thumb domain, respectively. (B) The detailed map of proposed pharmacophore. The contact residues in the pharmacophore map were displayed with the possible inhibitor binding site. The red stick, blue stick, and green sphere represent the hydrogen bond acceptor, hydrogen bond donor, and hydrophobic interaction site of ligand, respectively.

compounds that exhibit unfavorable interactions with the binding site or those that adopt unrealistic conformations on pharmacophore mapping were removed by visual inspection. Further filtering out the primary screened compounds using diversity analysis, we obtained 119 compounds for further testing in vitro.

2.3. In vitro screening of inhibitors

We then investigated whether the virtually screened 119 candidates inhibit RdRp activity in vitro. Most compounds were dissolved in 100% dimethyl sulfoxide (DMSO, Sigma). Some compounds that were not easily dissolved in DMSO were excluded from in vitro inhibition assay. We initially investigated the inhibitory effects of candidate compounds at the concentration of 100 μM. The RdRp reaction was performed using homopolymeric template and appropriate primer as described in Section 4, and the reaction products were resolved by 5% PAGE-7 M urea and visualized under Phosphor imager (Fig. 2). Through the first in vitro screening, seven compounds (CVP09008, 11, 19, 29, 47, 81, 111) were initially shown to significantly inhibit the RdRp activity. The inhibitory effects of the seven compounds on the RdRp activity were repeatedly tested, enabling us to select the final three compounds (CVP09011, CVP09047, and CVP09081 in Table

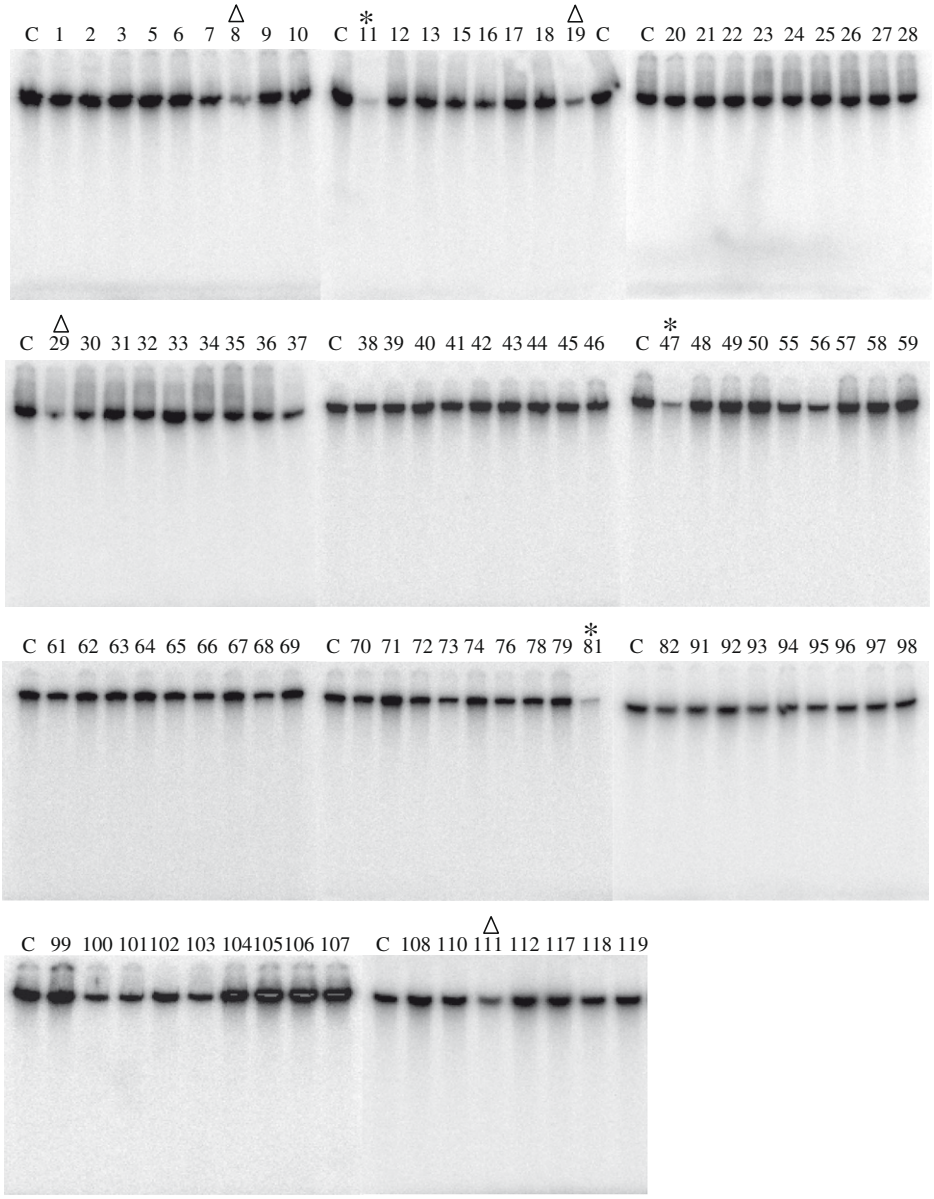

Figure 2. In vitro screening of inhibitor candidates. Inhibition of HCV NS5B RdRp activity by the virtually screened compounds (100 μM) was investigated by measuring the incorporated [α-^{32}P]UTP in the RdRp assay (see Section 4). These reaction mixtures were resolved by 5% PAGE gel containing 7 M Urea. After gel drying, the amount of radiolabeled RNA polymer was measured using the Phosphor imager. The compounds of CVP09011, CVP09047, and CVP09081 were screened (*) whereas compounds CVP09008, CVP09019, CVP09029, and CVP09111 were identified as false positive (△) by the repeated test (data not shown).

1). These compounds have shown to exhibit more than 80% inhibition at 100 μM. We tested RdRp activity at different treatment times (1 h, 2 h, and 3 h) where we could not find significant differences in inhibition activity (data not shown). Therefore, we used 2 h for routine RdRp activity assay. Then reactions were performed on serial dilution of inhibitors in DMSO (100, 50, 20, 10, 5 μM), and the 50% inhibitory concentration (IC_{50}) was determined. All three compounds were found to inhibit NS5B polymerase activity in a

Table 1
Chemical structure and IC_{50} value of the novel inhibitors

Compound	CVP09011	CVP09047	CVP09081
Structure	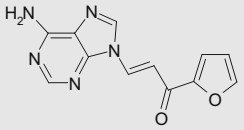	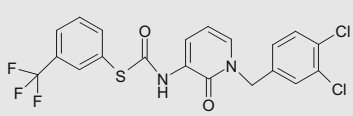	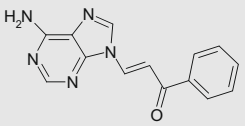
IC_{50} (μM)[a]	20 ± 5	20 ± 5	20 ± 5

[a] Values from at least three independent experiments.

dose-dependent manner. From three independent experiments, the IC_{50} value of CVP09011, CVP09047, and CVP09081 was estimated as about 20 μM (Fig. 3).

2.4. Mode of inhibition

Because the novel inhibitors reported here were screened for allosteric binding pocket of HCV NS5B, they were expected to function in a manner different from competitive inhibitors that are targeted to active site. To determine inhibition mode of CVP09011, CVP09047, and CVP09081, the RdRp reaction were performed in which the concentration of UTP was varied. With the RdRp assay results of varied UTP substrate concentrations (1, 2, 5, 10 μM) and inhibitor concentrations (0, 20, 50, 100 μM), we obtained a double-reciprocal plot (Fig. 4). The Km value for UTP substrate was about 2 μM in our in vitro assay setting and similar to previous reports.[43,44] In accordance with our prediction, all three compounds act primarily in a noncompetitive manner with respect to UTP.

2.5. Construction of NS5B mutants

We next constructed single-point mutants in the binding pocket to investigate whether the residues, apart from the catalytic center, affect the RdRp activity. The binding pocket includes the following residues such as Pro 197, Arg 200, Val 201, Cys 366,

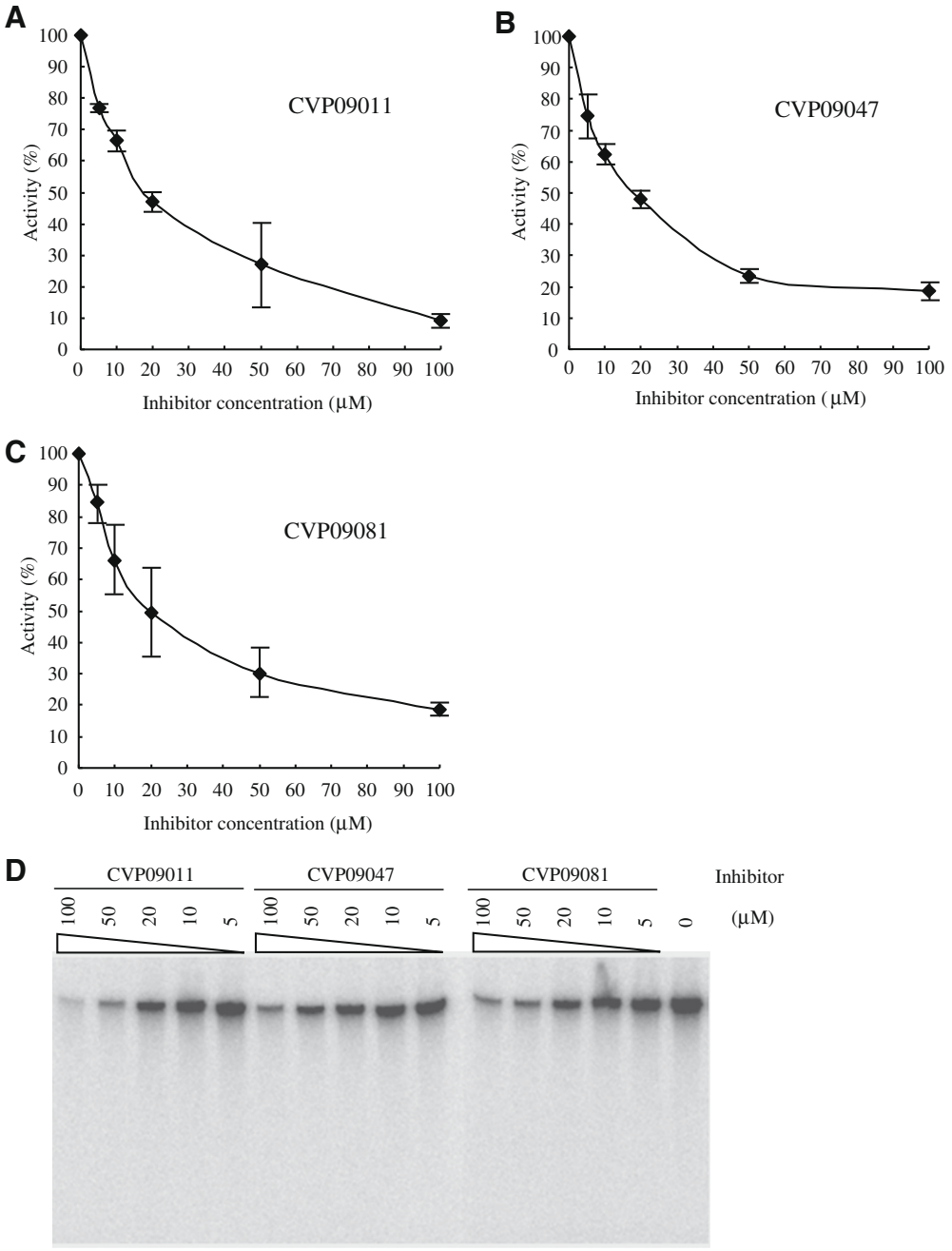

Figure 3. Dose-dependent inhibition by the lead compounds. The inhibition level on the HCV NS5B by the compounds CVP09011 (A), CVP09047 (B), and CVP09081 (C), respectively, were tested with various inhibitor concentrations ranging from 0 to 100 μM. The RdRp reaction mixture was resolved with 7 M urea 5% PAGE and visualized by BAS2500 (D). With the visualized image data of the three independent experiments, the RdRp activity was quantified by Image Gauge software (A, B, C). The error bars are standard deviations.

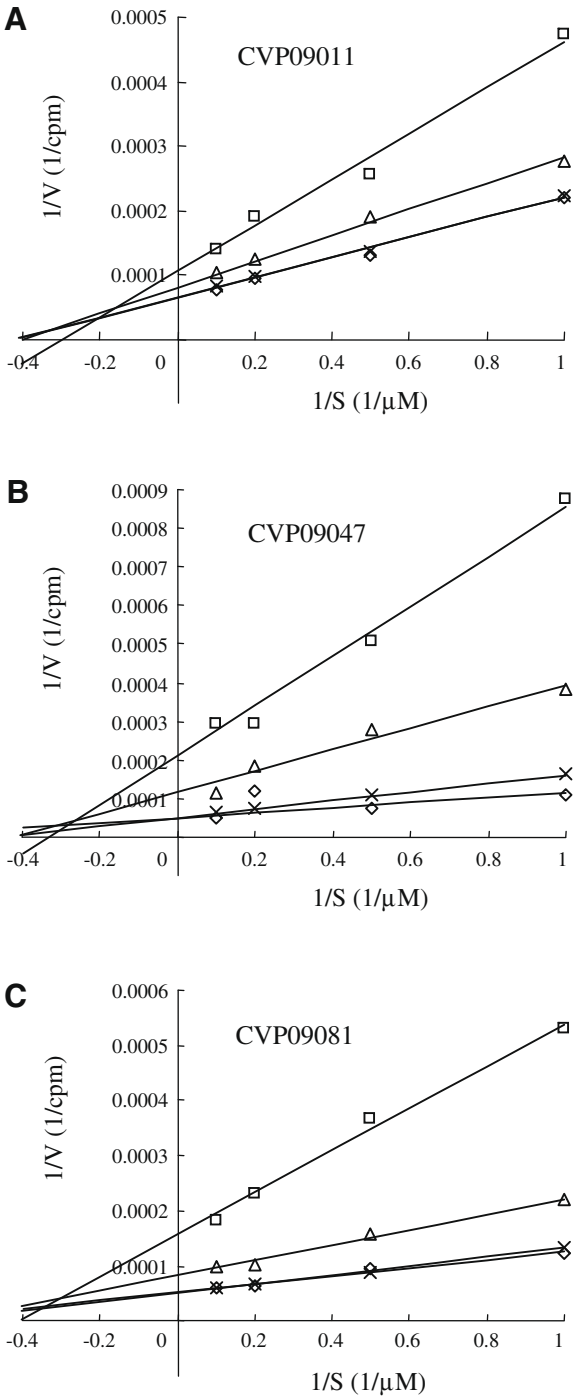

Figure 4. Kinetic analysis of inhibition of the RdRp activity by the lead compounds. The double-reciprocal plots of CVP09011 (A), CVP09047 (B), and CVP09081 (C) were obtained using the following procedure. The RdRp reaction was performed in various substrate concentration of UTP (1–10 μM). The reaction mixture was precipitated at cellulose filter and washed three times with 10% TCA solution containing 20 mM sodium diphosphate. The incorporated [α-^{32}P]UTP was measured by the liquid scintillation counter LS6500 and the results are displayed as double-reciprocal plot. The test inhibitor concentration was 0–100 μM (0 μM: ◇, 20 μM: ×, 50 μM: △, 100 μM: □). The inhibition mode was predominantly noncompetitive.

Ser 368, Val 381, Tyr 382, Leu 384, Met 414, Tyr 415, Leu 466, His 467, and Ser 470. From the amino acid sequence alignment, most of residues in the binding pocket were found to be highly conserved in all genotypes except for Val 381, Met 414, and Ser 470 (Table 2). We generated each single-point mutant with six residues

Table 2
Conservation of the residues in the binding pocket of HCV NS5B

Genotype	Arg 200	Cys 366	Ser 368	Leu 384	Tyr 415	His 467
Type 1a	R	C	S	L	F	H
Type 1b	R	C	S	L	Y(F)[a]	H
Type 2a	R	C	S	L	Y	H
Type 2b	R	C	S	L	Y	H
Type 3a	R	C	S	L	Y	H
Type 4a	R	C	S	L	Y	H
Type 5a	R	C	S	L	Y	H
Type 6a	R	C	S	L	F	H

[a] Most of genotype 1b clones have tyrosine residue at 415, but in some cases have residue of phenylalanine at this site.

(Arg 200, Cys 366, Ser 368, Leu 384, Tyr 415, and His 467) replaced by alanine. All mutants were expressed as soluble form in *E. coli* and purified as near homogeneity (data not shown). As shown in Figure 5, the RdRp activity of most mutants significantly decreased as compared with that of wild type NS5B (Wt); the RdRp activity of R200A, C366A, L384A, Y415A, and H467A were 48%, 51%, 25%, 0%, and 5% of wild type, respectively. The only exception was the S368A mutant, where no significant effect on activity was observed. The results indicate that the conserved residues in the binding pocket are generally important for RdRp activity of NS5B, suggesting that the selected binding pocket in this study could be an ideal pharmacophore for inhibitor target.

3. Discussion

In the present study, we have identified novel inhibitors of HCV NS5B through the virtual screening and the in vitro RdRp assay. Despite the seriousness of HCV infection worldwide, vaccine has not been so far available for the prevention or treatment of HCV infection due to the high degree of strain variation. Currently, the anti-HCV therapy is based primarily on the prescription of interferon-α only or the combination with ribavirin, a nucleoside analog. However, relatively low therapeutic effects and associated adverse side-effects compromised the effectiveness of these therapies,[18,30] requiring the development of more effective and safer anti-HCV agents.

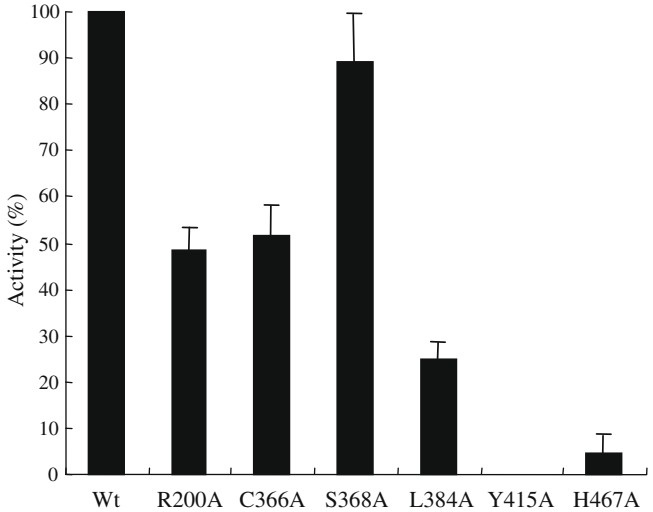

Figure 5. The effect of the binding pocket mutation on the RdRp activity. The wild type HCV NS5B and its six variants carrying each single-point mutation in the binding pocket were expressed, purified, and their RdRp activity was assayed as described in Section 4. The RdRp activities of mutants were obtained from three independent experiments and compared as relative to that of wild type (100%).

The pharmacophore, which is illustrated in Figure 1, is distinct from the binding pocket for nucleotide substrates in RNA polymerization, enabling us to perform the virtual screening for novel inhibitors. As shown in Table 2, the amino acid residues around the new pharmacophore are highly conserved among all HCV genotypes. Therefore, the pharmacophore model derived from our study using the HCV genotype 1b would be relevant for the generation of antivirals for all HCV genotypes. Moreover, the mutagenesis of the conserved residues (Fig. 5) indicates that this region is important for the overall function of RdRp activity of NS5B. The mutation of Y415A and H467A almost completely abrogated the polymerization activity while the mutation of R200A, C366A, and L384A significantly decrease it. The only mutant that failed to decrease the polymerase activity significantly is the S368A mutation, and it is interesting to note that this mutation is associated with antiviral resistance to nonnucleoside inhibitor in the replicon cell.[45] Considering the crucial role of Y415 and H467 residue, the inhibitors targeted to these residues would be most effective. The high degree of conservation, functional importance, and the pocket distinct from the catalytic center suggest that the newly identified binding pocket in this study could be one of the promising target sites for the development of effective anti-HCV agents. While we proposed and used this pharmacophore, located in interface between thumb and palm domains, for novel inhibitor identification, there have been significant advances on development of nonnucleoside analogs. With the crystal structure of inhibitor and NS5B complex, four potential allosteric sites were recently discovered.[20,24] One of promising allosteric binding site is located in the interface between palm and thumb domains, similar to our proposed pharmacophore.[26,31,33] They showed that the binding pocket is consisted of residues such as Pro 197, Arg 200, Leu 384, Met 414, and Tyr 448. In our model, the pocket would be consisted of residues including Pro 197, Arg 200, Val 201, Cys 366, Ser 368, Tyr 383, Leu 384, Met 414, Tyr415, His 467, and Tyr 448. While consistent with previously identified binding pocket, our result further shows an extended hydrophobic pocket composed of Val 201, Tyr 383, Leu 384, and His 467. It is likely that the action mode of the inhibitors binding to the new pharmacophore is different from that of nucleoside analogs, which are broadly used in the anti-viral therapy. All three compounds selected here in our study inhibited the RdRp activity primarily in noncompetitive manner with respect to UTP, as shown in Figure 4. Most of nonnucleoside analogs do not inhibit human DNA polymerase and therefore would exhibit lower toxicity as compare to nucleoside analogs. These inhibitors could also be used for the combination therapy with other discovered or used inhibitors.

Using the pharmacophore distinct from the active site, we screened the candidate compounds in silico, for which inhibitory function was confirmed in vitro. Through in silico screening, the test compounds were down-sized from 3.5 million to 119. From the pool of compounds tested in vitro, three compounds (CVP09011, CVP09047, and CVP09081) exhibited the IC_{50} values of about 20 μM. Their chemical structures were illustrated in Table 1. Notably, the structure of CVP09011 and CVP09081 are similar to each other, both carrying adenine moiety and a side chain of similar length and chemical structure at N_9 position. As shown in Figure 6A, the adenine moiety could make hydrogen bond with the side chains of Ser 368, Tyr 415, and Tyr448. The furan ring of CVP09011 and benzene ring of CVP09081 could make interactions with the side chains of Pro 197, Val 201, Tyr 383, Leu 384, and His 467 by hydrophobic interaction. In the case of CVP09047, the carbonyl group of pyridinone ring could have hydrogen bond with the side chains of Ser 368 and Tyr 415 (Fig. 6B). The 3-trifluoro-methyl benzene substituent is accessible to make interactions with the side chains of Pro 197, Val 201, Tyr 383, Leu 384, and His 467 by hydrophobic interaction. Additionally, the 3,4-dichloro-benzyl moiety could make a hydrophobic interaction with Tyr 448. The similarity in superimposed docking model of CVP09011 and CVP09047 probably demonstrate the similar IC_{50} value among three inhibitors of different scaffold. The IC_{50} values of initial leads

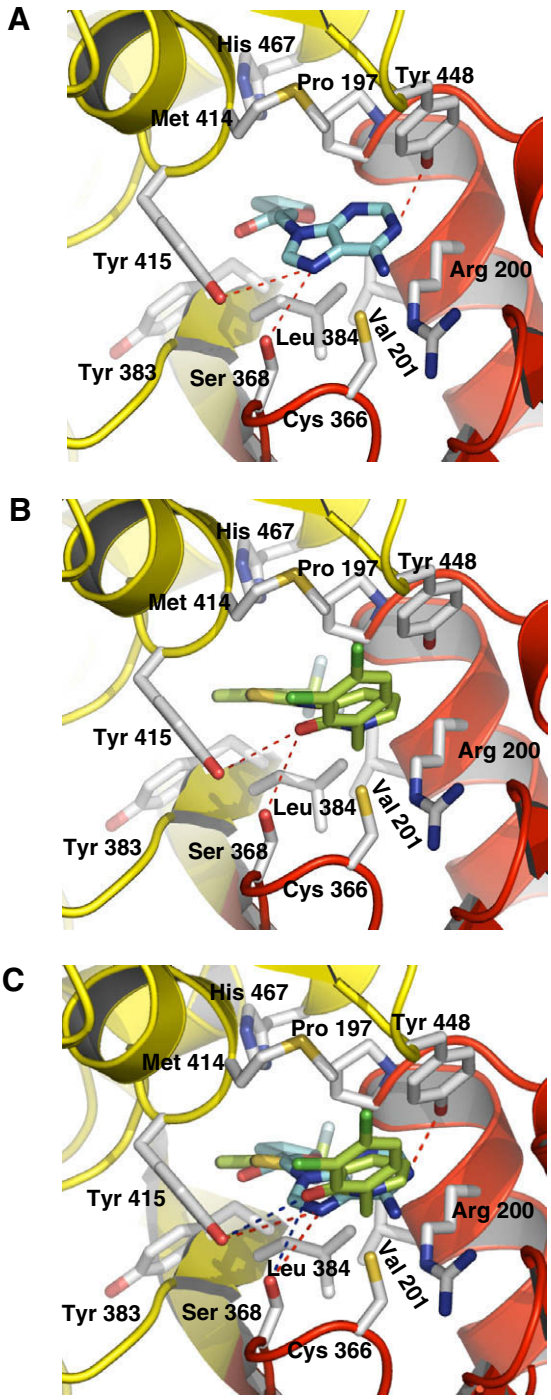

Figure 6. A refined docking model of CVP09011 and CVP09047 at the allosteric site of NS5B. The refined docking model of CVP09011 (A) and CVP09047 (B) into HCV NS5B was performed with version 4.0 of the AUTODOCK program. The CVP09011 and CVP09047 binding pocket is located near the primer-grip site of HCV NS5B (Cys 366 and Ser 367). The hydrogen bond between the 6-amino-purine moiety of CVP09011 and the side chains of Ser 368, Tyr 415, and Tyr 448 are represented as red dotted line. And also, the hydrogen bond between the CVP09047 and the side chains of Ser 368 and Tyr 415 are indicated as red dotted line. (C) Superimposed docking model of CVP09011 and CVP09047. Different colors are used to indicate the hydrogen bond between the compounds and NS5B residues (red for CVP09011, blue for CVP09047).

could be further improved by structure–activity relationship studies in combination with chemical synthesis of derivatives. Previously, HTS has been usefully employed for identification of anti-HCV agents, for example, benzo-1,2,4-thiadiazine as screened from GlaxoSmithKline proprietary compound collection,[21] or novel racemic inhibitor identified from the Pfizer proprietary compound archive.[32] In parallel with HTS from chemical libraries, the combination of virtual screening and in vitro confirmation of inhibitory activity would significantly expedite the process of identifying potential therapeutic entities.

It is important to consider how the identified inhibitors bound to the pocket inhibit the activity of RdRp. On the basis of the crystal structure of HCV NS5B,[14] the proposed binding pocket is located about 15 Å from the binding site of nucleoside substrate but it is in close proximity to the primer binding site. Here, the local structures of the complexes of NS5B-CVP09011 and CVP09047 were generated with the docking simulation (Fig. 6). It is likely that the binding of the inhibitor at the allosteric site could affect the binding of substrate at the active site or primer binding via steric hindrance. Further studies on the crystal structure of the complex of NS5B-inhibitor would unambiguously reveal the action mechanisms of the inhibitors presented here. In this study, we performed the virtual screening of the inhibitors that fit a pharmacophore distinct from the active site of NS5B and discovered the novel inhibitors by confirming the activity in an in vitro RdRp assay. These inhibitors and the pharmacophores may provide a platform to further screen related compounds for improved activities, and merit further investigation at preclinical and clinical level as potentially effective anti-HCV agents.

4. Experimental

4.1. Virtual screening

To search for the possible HCV NS5B inhibitor, we analyzed the proposed template-primer complex model of HCV NS5B for viral replication and rearrangement of the thumb domain upon RNA binding.[14] The pharmacophore was analyzed using PharmoMap™, Equispharm's in-house software package for structure-based virtual screening.[42] The constructed pharmacophore models were the feature-based in which the pharmacophoric points are represented by chemical features, such as hydrogen bond acceptors/donors or hydrophobic features. The pharmacophore models were employed as search query to identify HCV NS5B binding site target inhibitors from a 3-D small molecule database, which is commercially available multi-conformer three-dimensional database of 3.5 million compounds (PharmoDB™). The structure-based virtual screening for possible HCV inhibitor binding pocket of NS5B was carried out using the PharmoScan™ (Equispharm, Korea). The pharmacophore-based virtual screening hit compounds that exhibited unfavorable interactions with the binding site or adopted unrealistic conformations were filtered out by visual inspection.

4.2. Molecular docking

For a refined docking model of virtual screened hit compound (CVP09011) into the HCV NS5B, automated docking simulation was performed with version 4.0 of the program AUTODOCK.[46] The X-ray crystal structure of NS5B of HCV genotype 1b from Protein Data Bank (PDB code 2AX0) was used for our docking simulation.[36] An initial protein structure was energy-minimized for 1000 steps employing steepest descent algorithm by using Discover version of 2.98 of Insight II (Accelrys Inc., San Diego, CA). For docking, the structure HCV NS5B was kept rigid whereas all the torsional bonds in CVP09011 were set free to perform flexible docking. The binding energy between protein and CVP09011 was evaluated using atom affinity potentials that are pre-calculated on a grid maps calculated using AutoGrid. The grid maps had dimensions of 60 * 60 * 60 Å with 0.375 Å spacing between grid points. In AUTODOCK4, docking was performed by combining a global genetic algorithm with local minimization, Lamarckian genetic algorithm. One hundred trials were preformed for each docking, and final docked conformations were clustered using a tolerance of 1 Å root-mean-square deviation (RMSD). The docking conformation properly oriented towards the HCV NS5B inhibitor binding pocket was selected, and the free energy of binding was estimated. The molecular graphics of selected possible HCV NS5B inhibitor binding pocket and refined docking model with lead compound was generated using PyMol package (http://pymol.sourceforge.net).

4.3. Expression and purification of HCV NS5B protein

For the in vitro screening of NS5B inhibitors, the C-terminal 21 amino acids truncated NS5B of genotype 1b carrying six consecutive histidine residues at its N-terminus was cloned under the control of T7 promoter. The overexpressed NS5B in *E. coli* was purified by Ni-affinity chromatography. With single step purification, we obtained the HCV NS5B with near homogeneity as judged by the SDS–PAGE. The purified protein concentration, determined by the BCA method and SDS–PAGE, was 313 ng/μl. The purified wild type NS5B exhibited RdRp activity and the enzyme activity was inhibited by the previously reported inhibitor benzo-1,2,4-thiadiazine (data not shown). This enzyme was used in an in vitro RdRp activity assay.

4.4. In vitro RdRp activity assay

The inhibitory effect of compounds on the HCV NS5B's RdRp activity was estimated using the radio-labeled UTP incorporation assay using homo poly-ribonucleotide. The compounds were tested in a total volume of 20 μl reaction mixture containing of 20 mM Tris–HCl, pH 6.8, 10 mM $MgCl_2$, 1 mM DTT, 10 mM KCl, 4 μg rifampicin, 20 U RNase inhibitor, 200 ng PolyrA/oligodT_{12-15} (Amersham Pharmacia Biotech), 10 μM cold UTP, 0.2 μCi [α-^{32}P]UTP (3000 Ci/mmol; NEN Life Science), and 62.7 ng (about 1 pmol) purified HCV NS5B. The RdRp reaction mixtures were incubated at 30 °C for 2 h. The reaction was terminated by the addition of equal volume of RNA loading buffer (80% formamide, 100 mM EDTA, 0.05% SDS, 0.025% bromophenol blue, and 0.025% xylene cyanol FF) followed by immediate boiling for 2 min. These mixtures were resolved on 5% PAGE gel containing 7 M urea. After exposure to imaging plate, the density of corresponding RNA product band was analyzed by Phosphor imager BAS2500 and Image Gauge v3.46 (Fuji Photo Film, Japan).

4.5. Kinetic analysis of enzyme inhibition

The RdRp reactions were performed with various concentrations of UTP (1–10 μM containing [α-^{32}P] UTP (corresponding to 0.2–2 μCi)). Then the reaction was repeated in the presence of each inhibitor and the inhibition mode for each candidate compounds was then evaluated by the double-reciprocal plot. The assay procedure was same as previously described with some modification at the quantification protocols. The RdRp reaction mixtures were precipitated at cellulose filter Grade 2 (Whatman) that was presoaked and dried with 15% TCA solution (Sigma). After washing of unincorporated nucleotides with 10% TCA solution containing 20 mM sodium diphosphate, the cellulose filters were dried and the radioactivity was quantified by the liquid scintillation counter LS6500 (Beckman Coulter).

Acknowledgements

This work was supported in part by the Korea Science and Engineering Foundation (KOSEF) Grant (Grant No. 2007-04384), the Korea Research Foundation Grant (Grant No. KRF-2004-005-C00148), and Second-phase of BK21 Project in 2009 (to K.H. Kim) by the Korean Government.

References and notes

1. Choo, Q. L.; Kuo, G.; Weiner, A. J.; Overby, L. R.; Bradley, D. W.; Houghton, M. *Science* **1989**, *244*, 359.
2. Wasley, A.; Alter, M. J. *Semin. Liver Dis.* **2000**, *20*, 1.
3. Lindenbach, B. D.; Rice, C. M. In *Field's Virology*; Fields, B. N., Knipe, D. M., Howley, P. M., Eds.; Lippincott Williams & Wilkins, 2001; pp 991–1024.
4. Rosenberg, S. *J. Mol. Biol.* **2001**, *313*, 451.
5. Lévêque, V. J. P.; Wang, Q. M. *Cell. Mol. Life Sci.* **2002**, *59*, 909.
6. Walker, M. P.; Hong, Z. *Curr. Opin. Pharmacol.* **2002**, *2*, 534.
7. Hong, Z.; Cameron, C. E.; Walker, M. P.; Castro, C.; Yao, N.; Lau, J. Y.; Zhong, W. *Virology* **2001**, *285*, 6.
8. Schmidt-Mende, J.; Bieck, E.; Hugle, T.; Penin, F.; Rice, C. M.; Blum, H. E.; Moradpour, D. *J. Biol. Chem.* **2001**, *276*, 44052.
9. Behrens, S. E.; Tomei, L.; De Francesco, R. *EMBO J.* **1996**, *15*, 12.
10. Ferrari, E.; Wright-Minogue, J.; Fang, J. W.; Baroudy, B. M.; Lau, J. Y.; Hong, Z. *J. Virol.* **1999**, *73*, 1649.
11. Lohmann, V.; Korner, F.; Herian, U.; Bartenschlager, R. *J. Virol.* **1997**, *71*, 8416.
12. Oh, J. W.; Ito, T.; Lai, M. M. C. *J. Virol.* **1999**, *73*, 7694.
13. Ago, H.; Adachi, T.; Yoshida, A.; Yamamoto, M.; Habuka, N.; Yatsunami, K.; Miyano, M. *Struct. Fold Des.* **1999**, *7*, 1417.
14. Bressanelli, S.; Tomei, L.; Roussel, A.; Incitti, I.; Vitale, R. L.; Mathieu, M.; De Francesco, R.; Rey, F. A. *Proc. Natl. Acad. Sci. U.S.A.* **1999**, *96*, 13034.
15. Lesburg, C. A.; Cable, M. B.; Ferrari, E.; Hong, Z.; Mannarino, A. F.; Weber, P. C. *Nat. Struct. Biol.* **1999**, *6*, 937.
16. De Clercq, E. J. *Clin. Virol.* **2001**, *22*, 73.
17. Pramoolsinsup, C. *J. Gastroenterol. Hepatol.* **2002**, *17*, S125.
18. McHutchison, J. G.; Gordon, S. C.; Schiff, E. R.; Shiffman, M. L.; Lee, W. M.; Rustgi, V. K.; Goodman, Z. D.; Ling, M. H.; Cort, S.; Albrecht, J. K. *N. Engl. J. Med.* **1998**, *339*, 1485.
19. Carroll, S. S.; Tomassini, J. E.; Bosserman, M.; Getty, K.; Stahlhut, M. W.; Eldrup, A. B.; Bhat, B.; Hall, D.; Simcoe, A. L.; LaFemina, R.; Rutkowski, C. A.; Wolanski, B.; Yang, Z.; Migliaccio, G.; De Francesco, R.; Kuo, L. C.; MacCoss, M.; Olsen, D. B. *J. Biol. Chem.* **2003**, *278*, 11979.
20. De Francesco, R.; Carfí, A. *Adv. Drug Delivery Rev.* **2007**, *59*, 1242.
21. Dhanak, D.; Duffy, K. J.; Johnston, V. K.; Lin-Goerke, J.; Darcy, M.; Shaw, A. N.; Gu, B.; Silverman, C.; Gates, A. T.; Nonnemacher, M. R.; Earnshaw, D. L.; Casper, D. J.; Kaura, A.; Baker, A.; Greenwood, C.; Gutshall, L. L.; Maley, D.; Del Vecchio, A.; Macarron, R.; Hofmann, G. A.; Alnoah, Z.; Cheng, H. Y.; Chan, G.; Khandekar, S.; Keenan, R. M.; Sarisky, R. T. *J. Biol. Chem.* **2002**, *277*, 38322.
22. Gu, B.; Johnston, V. K.; Gutshall, L. L.; Nguyen, T. T.; Gontarek, R. R.; Darcy, M. G.; Tedesco, R.; Dhanak, D.; Duffy, K. J.; Kao, C. C.; Sarisky, R. T. *J. Biol. Chem.* **2003**, *278*, 16602.
23. Howe, A. Y.; Bloom, J.; Baldick, C. J.; Benetatos, C. A.; Cheng, H.; Christensen, J. S.; Chunduru, S. K.; Coburn, G. A.; Feld, B.; Gopalsamy, A.; Gorczyca, W. P.; Herrmann, S.; Johann, S.; Jiang, X.; Kimberland, M. L.; Krisnamurthy, G.; Olson, M.; Orlowski, M.; Swanberg, S.; Thompson, I.; Thorn, M.; Del Vecchio, A.; Young, D. C.; van Zeijl, M.; Ellingboe, J. W.; Upeslacis, J.; Collett, M.; Mansour, T. S.; O'Connell, J. F. *Antimicrob. Agents Chemother.* **2004**, *48*, 4813.
24. Koch, U.; Narjes, F. *Curr. Top. Med. Chem.* **2007**, *7*, 1302.
25. Louise-May, S.; Yang, W.; Nie, X.; Liu, D.; Deshpande, M. S.; Phadke, A. S.; Huang, M.; Agarwal, A. *Bioorg. Med. Chem. Lett.* **2007**, *17*, 3905.
26. Yan, S.; Appleby, T.; Gunic, E.; Shim, J. H.; Tasu, T.; Kim, H.; Rong, F.; Chen, H.; Hamatake, R.; Wu, J. Z.; Hong, Z.; Yao, N. *Bioorg. Med. Chem. Lett.* **2007**, *17*, 28.
27. Zhong, W.; An, H.; Barawkar, D.; Hong, Z. *Antimicrob. Agents Chemother.* **2003**, *47*, 2674.
28. Le Pogam, S.; Jiang, W. R.; Leveque, V.; Rajyaguru, S.; Ma, H.; Kang, H.; Jiang, S.; Singer, M.; Ali, S.; Klumpp, K.; Smith, D.; Symons, J.; Cammack, N.; Nájera, I. *Virology* **2006**, *351*, 349.
29. Migliaccio, G.; Tomassini, J. E.; Carroll, S. S.; Tomei, L.; Altamura, S.; Bhat, B.; Bartholomew, L.; Bosserman, M. R.; Ceccacci, A.; Colwell, L. F.; Cortese, R.; De Francesco, R.; Eldrup, A. B.; Getty, K. L.; Hou, X. S.; LaFemina, R. L.; Ludmerer, S. W.; MacCoss, M.; McMasters, D. R.; Stahlhut, M. W.; Olsen, D. B.; Hazuda, D. J.; Flores, O. A. *J. Biol. Chem.* **2003**, *278*, 49164.
30. Moore, M. M.; Elpern, D. J.; Carter, D. J. *Arch. Dermatol.* **2004**, *140*, 215.
31. Gopalsamy, A.; Chopra, R.; Lim, K.; Ciszewski, G.; Shi, M.; Curran, K. J.; Sukits, S. F.; Svenson, K.; Bard, J.; Ellingboe, J. W.; Agarwal, A.; Krishnamurthy, G.; Howe, A. Y.; Orlowski, M.; Feld, B.; O'Connell, J.; Mansour, T. S. *J. Med. Chem.* **2006**, *49*, 3052.
32. Love, R. A.; Parge, H. E.; Yu, X.; Hickey, M. J.; Diehl, W.; Gao, J.; Wriggers, H.; Ekker, A.; Wang, L.; Thomson, J. A.; Dragovich, P. S.; Fuhrman, S. A. *J. Virol.* **2003**, *77*, 7575.
33. Nittoli, T.; Curran, K.; Insaf, S.; DiGrandi, M.; Orlowski, M.; Chopra, R.; Agarwal, A.; Howe, A. Y.; Prashad, A.; Floyd, M. B.; Johnson, B.; Sutherland, A.; Wheless, K.; Feld, B.; O'Connell, J.; Mansour, T. S.; Bloom, J. *J. Med. Chem.* **2007**, *50*, 2108.
34. Wang, M.; Ng, K. K.; Cherney, M. M.; Chan, L.; Yannopoulos, C. G.; Bedard, J.; Morin, N.; Nguyen-Ba, N.; Alaoui-Ismaili, M. H.; Bethell, R. C.; James, M. N. *J. Biol. Chem.* **2003**, *278*, 9489.
35. Ouyang, G.; Chen, Z.; Cai, X. J.; Song, B. A.; Bhadury, P. S.; Yang, S.; Jin, L. H.; Xue, W.; Hu, D. Y.; Zeng, S. *Bioorg. Med. Chem.* **2008**, *16*, 9699.
36. Powers, J. P.; Piper, D. E.; Li, Y.; Mayorga, V.; Anzola, J.; Chen, J. M.; Jaen, J. C.; Lee, G.; Liu, J.; Peterson, M. G.; Tonn, G. R.; Ye, Q.; Walker, N. P.; Wang, Z. *J. Med. Chem.* **2006**, *49*, 1034.
37. Tedesco, R.; Shaw, A. N.; Bambal, R.; Chai, D.; Concha, N. O.; Darcy, M. G.; Dhanak, D.; Fitch, D. M.; Gates, A.; Gerhardt, W. G.; Halegoua, D. L.; Han, C.; Hofmann, G. A.; Johnston, V. K.; Kaura, A. C.; Liu, N.; Keenan, R. M.; Lin-Goerke, J.; Sarisky, R. T.; Wiggall, K. J.; Zimmerman, M. N.; Duffy, K. J. *J. Med. Chem.* **2006**, *49*, 971.
38. Yan, S.; Appleby, T.; Larson, G.; Wu, J. Z.; Hamatake, R. K.; Hong, Z.; Yao, N. *Bioorg. Med. Chem. Lett.* **2007**, *17*, 1991.
39. Corbeil, C. R.; Englebienne, P.; Yannopoulos, C. G.; Chan, L.; Das, S. K.; Bilimoria, D.; L'heureux, L.; Moitessier, N. *J. Chem. Inf. Model.* **2008**, *48*, 902.
40. Lyne, P. D. *Drug Discovery Today* **2002**, *7*, 1047.
41. Smith, R. M.; Wu, G. Y. *J. Viral Hepatitis* **2003**, *10*, 405.
42. Kim, D. Y.; Kim, K. H.; Kim, N. D.; Lee, K. Y.; Han, C. K.; Yoon, J. H.; Moon, S. K.; Lee, S. S.; Seong, B. L. *J. Med. Chem.* **2006**, *49*, 5664.
43. Luo, G.; Hamatake, R. K.; Mathis, D. M.; Racela, J.; Rigat, K. L.; Lemm, J.; Colonno, R. J. *J. Virol.* **2000**, *74*, 851.
44. Tomei, L.; Vitale, R. L.; Incitti, I.; Serafini, S.; Altamura, S.; Vitelli, A.; De Francesco, R. *J. Gen. Virol.* **2000**, *81*, 759.
45. Lu, L.; Dekhtyar, T.; Masse, S.; Pithawalla, R.; Krishnan, P.; He, W.; Ng, T.; Koev, G.; Stewart, K.; Larson, D.; Bosse, T.; Wagner, R.; Pilot-Matias, T.; Mo, H.; Molla, A. *Antiviral Res.* **2007**, *76*, 93.
46. Morris, G. M.; Goodsell, D. S.; Halliday, R. S.; Huey, R.; Hart, W. E.; Belew, R. K.; Olson, A. J. *J. Comput. Chem.* **1998**, *19*, 1639.